

Breakdown of the Dipole Approximation in Soft-X-Ray Photoemission

O. Hemmers, P. Glans, D.L. Hansen, H. Wang, S.B. Whitfield, and D.W. Lindle¹
R. Wehlitz, J.C. Levin, and I.A. Sellin²
R.C.C. Perera³

¹University of Nevada Las Vegas, Las Vegas, Nevada, 89154-4003

²University of Tennessee, Knoxville, Tennessee, 37996-1200

³Berkeley Lab, Berkeley California, 94720

A mainstay of angle-resolved photoemission is the (electric-) “dipole approximation,” which ignores all higher-order photon interactions, such as electric-quadrupole and magnetic-dipole effects, and predicts simple electron ejection patterns as a function of angle. In the dipole approximation, a single parameter, β , completely describes electron angular distributions as a function of the angle, θ , relative to the polarization, \mathbf{E} , of the ionizing radiation (Figure 1). The solidly colored regions in Figure 2 represent angle-dependent photoemission patterns (with the ejection probability in any direction proportional to the distance from the origin) for different values of β in its range from -1 to 2 . For these dipole-approximation patterns, the angular distribution is always symmetrical around \mathbf{E} and is isotropic for the special case of $\beta = 0$ (Figure 2a).

In the first step beyond the dipole approximation, higher-order photon interactions lead to nondipole effects in these patterns, described by two new parameters, δ and γ . A second angle, ϕ , relative to the propagation direction, \mathbf{k} , of the ionizing radiation (Figure 1), also comes into play, permitting forward–backward asymmetry. To demonstrate how significant nondipole effects can be for angular-distribution patterns, the dotted curves in Figs. 2b and 2c and all three curves in Fig. 2a exemplify extreme values for δ or γ . All curves show the same ejection probability along the y axis and in the y - z plane and also show large differences in the forward and backward directions.

To probe the limits of the dipole approximation, soft x-ray photoemission measurements on neon were made at Beamline 8.0. Two-bunch operation was necessary because electron kinetic energies were determined via time of flight (TOF), an efficient technique in which nearly all kinetic energies can be measured simultaneously. The extremely high flux from an ALS undulator was necessary

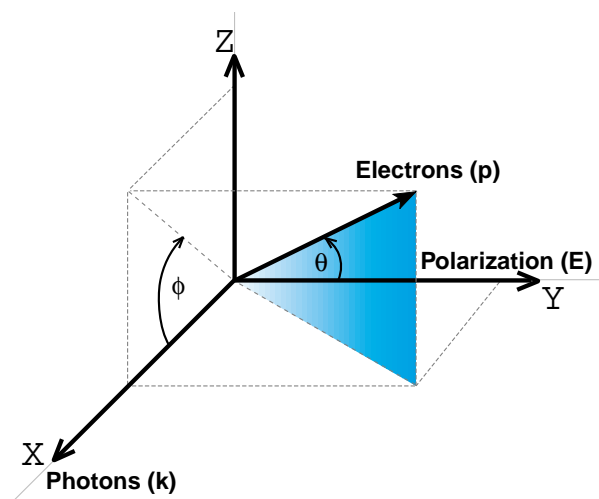


Figure 1. In the dipole approximation, β alone describes electron angular distributions as a function of the angle, θ , relative to the polarization, \mathbf{E} , of the radiation. Higher-order photon interactions lead to nondipole effects, described by two new parameters, δ and γ , and a second angle, ϕ , relative to the propagation direction, \mathbf{k} , of the radiation.

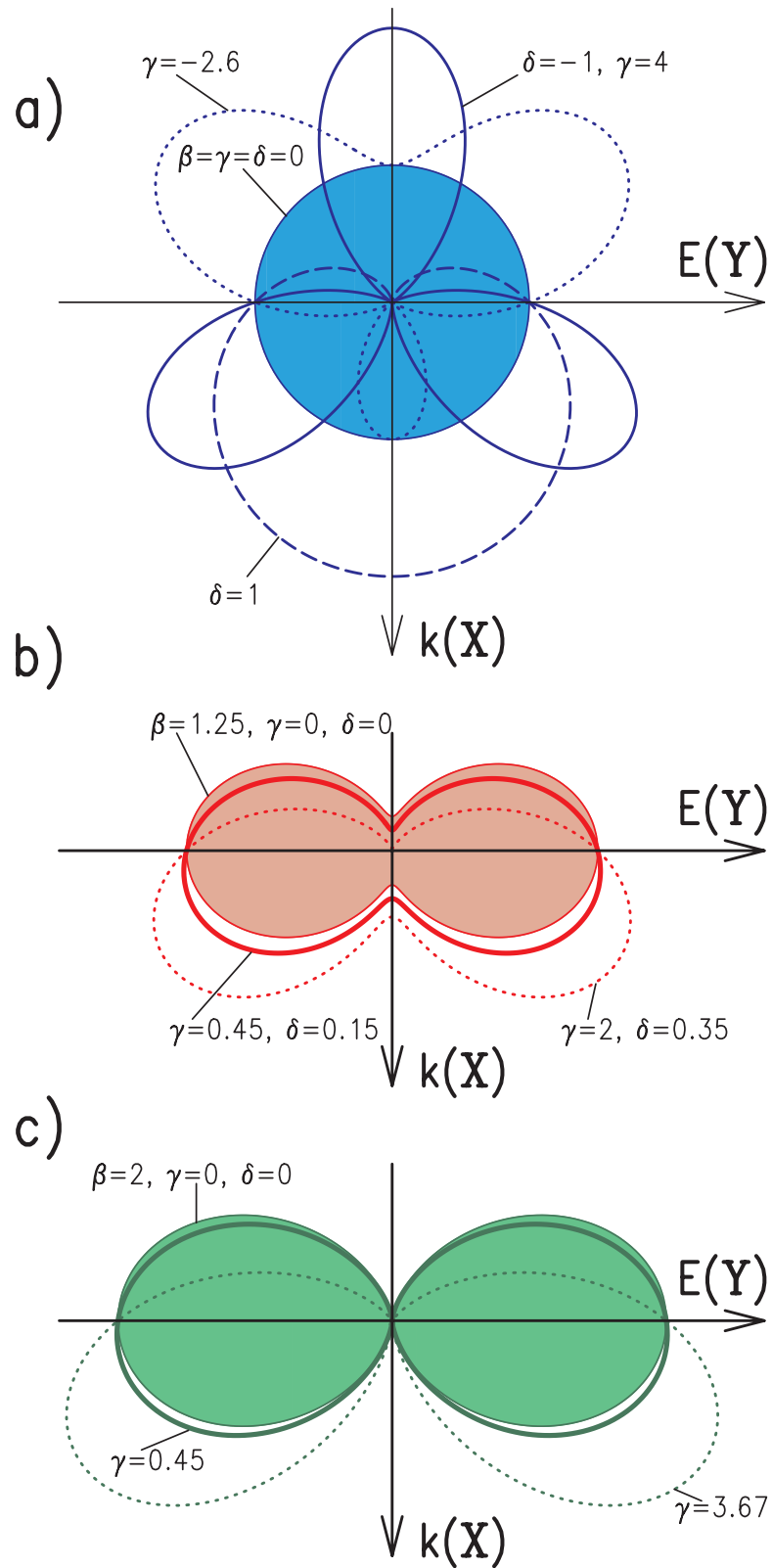


Figure 2. Angle-dependent photoemission patterns, with the ejection probability in any direction proportional to the distance from the origin. Solidly colored regions represent dipole-approximation patterns for different values of β . For these, the angular distribution is always symmetrical around \mathbf{E} and is isotropic for the special case of $\beta = 0$ (a). The solid curves in (b) and (c) represent nondipole angular-distribution patterns for 2p (b) and 2s (c) photoemission inferred from Figure 3.

to obtain sufficient signal for precise measurements of δ and γ . Two analyzers, placed at the “magic angle” ($\theta = 54.7^\circ$), where β has no influence, but at different angles ϕ to be sensitive to forward–backward asymmetries, sufficed to measure nondipole effects as a function of photon energy.

Figure 3 superimposes two neon photoemission spectra taken with the “magic-angle” analyzers, one in the y - z plane (light color), the other not (black). The spectra are scaled to each other by using neon *KLL* Auger lines, which must have isotropic angular distributions ($\beta = \delta = \gamma = 0$). Obvious intensity differences between the 2s and 2p photoemission peaks are due to nondipole effects. The solid curves in Figs. 2b and 2c represent nondipole angular-distribution patterns for 2p (b) and 2s (c) photoemission inferred from Figure 3. Other spectra show that intensity differences occur at energies as low as 250 eV. Changes in ejection probability as a function of angle are observable well below 1 keV, at photon energies much lower than generally expected for effects beyond the dipole approximation.

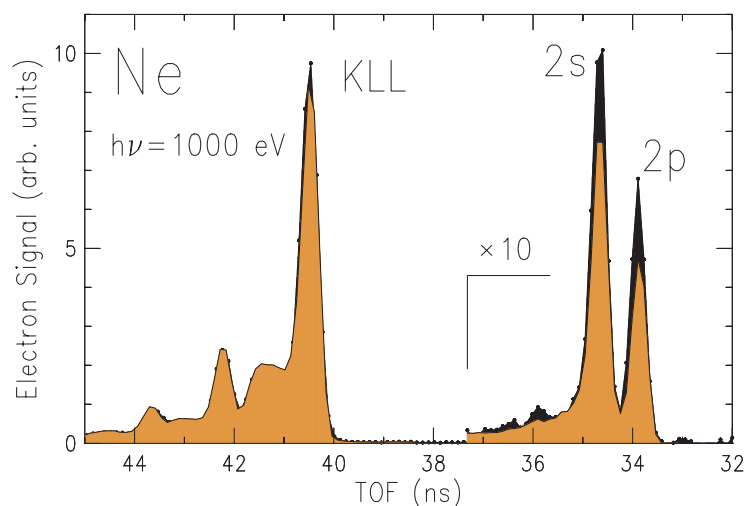


Figure 3. Superimposed neon photoemission spectra taken with the “magic-angle” analyzers, one in the y - z plane (light color), the other not (black). The spectra were scaled to each other by using neon *KLL* Auger lines. The intensity differences between the 2s and 2p photoemission peaks are due to nondipole effects.

More significantly, measurements on other atoms and molecules demonstrate that “low-energy” breakdown of the dipole approximation is a general phenomenon. It is likely that many applications of angle-resolved photoemission (e.g., most studies of atoms and molecules, band mapping in solids, photoelectron diffraction and holography, orientational studies of adsorbates, etc.) need to include nondipole effects in their analyses. More work to determine the range of validity of the dipole approximation is under way.

1. D.W. Lindle and O. Hemmers, *J. Electron Spectrosc.* **100** (to be published).
2. O. Hemmers et al., *J. Phys. B* **30**, L727 (1997).
3. O. Hemmers et al., *Synchr. Rad. News* **9** (6), 40 (1996) and erratum **10** (3), 21 (1997).
4. O. Hemmers et al., *Rev. Sci. Instrum.* **69**, 3809 (1998).

This work was supported by the National Science Foundation; U.S. Department of Energy, Experimental Program to Stimulate Competitive Research; Research Corporation; and The Petroleum Research Fund.

Principal Investigator: Dennis W. Lindle, Department of Chemistry, University of Nevada, Las Vegas.
Email: lindle@nevada.edu. Telephone: (702) 895-4426.